Astron. Astrophys. 357, 219–224 (2000)

ASTRONOMY AND ASTROPHYSICS

ISOCAM observations of the Chamaeleon I dark cloud⋆,⋆⋆,⋆⋆⋆

P. Persi[1], A.R. Marenzi[1], G. Olofsson[2], A.A. Kaas[2,12], L. Nordh[2], M. Huldtgren[2], A. Abergel[3], P. André[4], S. Bontemps[2,5], F. Boulanger[3], M. Burggdorf[6], M.M. Casali[7], C.J. Cesarsky[4], E. Copet[8], J. Davies[9], E. Falgarone[10], T. Montmerle[4], M. Perault[10], T. Prusti[6], J.L. Puget[3], and F. Sibille[11]

[1] Istituto Astrofisica Spaziale, CNR, Area di Ricerca Tor Vergata, Via del Fosso del Cavaliere, 00133 Roma, Italy (persi@saturn.ias.)
[2] Stockholm Observatory, 133 36 Saltsjöbaden, Sweden
[3] IAS, Université Paris XI, Orsay, France
[4] Service d'Astrophysique, CEA Saclay, Gif-sur-Yvette, France
[5] Observatoire de Bordeaux, Floirac, France
[6] ISO Data Centre, ESA Astrophysics Division, Villafranca del Castillo, Spain
[7] Royal Observatory, Blackford Hill, Edinburgh, UK
[8] DESPA, Observatoire Paris-Meudon, France
[9] Joint Astronomy Centre, Hawaii, USA
[10] ENS Radioastronomie, Paris, France
[11] Observatoire de Lyon, France
[12] Astrophysics Division of ESA, ESTEC, 2201 AZ Noordwijk, The Netherlands

Received 3 December 1999 / Accepted 29 February 2000

Abstract. We present the results of an ISOCAM survey of the Chamaeleon I dark cloud conducted in two broad-band filters at 6.7 and 14.3 μm. In an area of 0.59 sq.deg. we have detected a total of 282 mid-IR sources with 103 sources observed in both filters. Combining the ISOCAM observations with the I, J, and K_s data obtained with DENIS, we have found 108 pre-main-sequence (PMS) stars in the region, of which 34 were previously unidentified. Several of these newly discovered young stellar objects are relatively faint suggesting a population in Cha I of very low mass objects that probably includes brown dwarfs in their early contraction phases. Finally, most of the PMS stars show the spectral index computed between 2.2 and 14.3 μm typical of Class II sources. The luminosity function (LF) derived for our detected PMS stars is discussed.

Key words: stars: formation – stars: low-mass, brown dwarfs – stars: luminosity function, mass function – stars: pre-main sequence – infrared: stars

1. Introduction

The Chamaeleon I dark cloud is located in the southern hemisphere, and is part of a complex of three clouds. This nearby star formation region (D=160 pc; Whittet et al. 1997) has been, recently and in the past, object of a considerable amount of observations in different spectral regions in order to study the processes of formation of very low-mass stars. This is because of its proximity to the Sun, isolated location at a high Galactic latitude (b$\sim$ -16°), and relatively low extinction.

Studies of the stellar population in Cha I were conducted mainly on the basis of Hα and X-Ray surveys, near–IR observations and IRAS data (see i.e. Prusti et al. 1992; Gauvin & Strom 1992; Lawson et al. 1996 and Cambrésy et al. 1998). All these observations were limited to pre-main sequence (PMS) stars with masses higher than $\sim 0.3\ M_\odot$. To probe the physical properties of the cloud such as the initial mass function (IMF) we need to have a complete census of the stellar population including very low-mass stars near or below the hydrogen burning limit.

The presence of a very low-mass young stellar population toward the northern and densest part of the Cha I dark cloud was found by Persi et al. (1999) using deep–near–IR images associated with ISOCAM observations. A very deep objective prism survey in the Hα of a small region of the center of Cha I ($\sim$ 100 arcmin^2) obtained by Comerón et al. (1999) detected six new very young objects with stellar luminosities in the range 0.02–0.08 $L_\odot$. These objects, according to the authors, do not show any infrared excess detectable in the K-band. Therefore, very deep near-IR surveys do not suffice for the detection of young objects near or below the hydrogen burning limit.

A method to detect very low mass stars in nearby clouds is represented by the survey carried out in two broad-band filters,

Send offprint requests to: P. Persi

⋆ ISO is an ESA project with instruments funded by ESA Member States (especially the PI countries: France, Germany, the Netherlands and the United Kingdom) and with the participation of ISAS and NASA.

⋆⋆ Tables 1 and 2 are only available in electronic form at the CDS via anonymous ftp to cdsarc.u-strasbg.fr (130.79.128.5) or via http://cdsweb.u-strasbg.fr/Abstract.html

⋆⋆⋆ Tables 3 and 4 are only available with the on-line publication at http://link.springer.de/link/service/journals/00230/

Correspondence to: Istituto Astrofisica Spaziale, CNR, Area di Ricerca Tor Vergata, Via del Fosso del Cavaliere, 00133, Roma, Italy

LW2(5–8.5 μm) and LW3(12–18 μm) obtained with the infrared camera (ISOCAM, Cesarsky et al. 1996) aboard of the ISO satellite (Kessler et al. 1996) (see i.e. Nordh et al. 1998; Olofsson et al. 1999). The advantage of mid-IR observations in searching for low mass young stellar objects is due to the fact that these young stars, surrounded by dust during their early contraction phases, ehibit mid-IR excesses which can be observationally separated from the effects of interstellar reddening. This dust emission is sometimes difficult to be detected in the near-IR.

ISOCAM observations have been used by Bontemps et al. (1999) to extend the study of the luminosity function (LF) of the ρ Oph cloud down to $L_\star \sim 0.05 L_\odot$, while Olofsson et al. (1999) find evidence for a population of very low mass stars in RCrA which are probably brown dwarfs in their early contraction phases.

In this paper, we report the results of the ISOCAM survey of the Cha I dark cloud. Preliminary results including this region were described by Nordh et al. (1996). In Sect. 2 observational details are given together with a brief description of the data analysis. We present in Sect. 3 the ISOCAM colour/magnitude and colour/colour diagrams obtained combining the ISOCAM data with the DENIS near–infrared photometry in order to search for new members of the cloud. Finally in Sect. 4 we present the luminosity function derived for all the observed members of Cha I.

2. Observations and data reduction

As part of the ISOCAM central program, nearby star formation regions were surveyed in the two broad band filters LW2(5–8.5 μm) and LW3(12–18 μm) (L_NORDH.SURVEY_1_2). Chamaeleon I was mapped in 5 separate, but overlapping main rasters for a total of 0.59 sq.deg. The outline of the observed region is given in Fig. 3. Each raster was made by scanning always along the right ascension with 90″overlap in right ascension and 24″overlap in declination. All the regions except the south-east were mapped with a pixel field of view (PFOV) of 6″, intrinsic integration time T_{int}= 2.1 s, and $\sim$ 15 s integration time per sky position. In order to avoid saturation the south-east region was observed with a PFOV=3″and T_{int}=0.28 s. The same T_{int} was used for the northern part of Cha I.

The raw data were processed using the CIA (v3.0) software (Ott et al. 1997). A general description of ISOCAM data processing is reported by Starck et al. (1999). The dark current of each frame was subtracted using the CAL-G dark current from the ISOCAM calibration library, while cosmic ray hits were detected and masked using the multiresolution median trasform (MMT) method (Starck et al. 1996). The transients due to detector memory effects were corrected with the inversion method described by Abergel et al. (1996). Finally the images were flat-fielded with a flat image constructed by median filtering the observations on the target field.

We have used an interactive IDL point source detection and photometry programme, developed for ISOCAM rasters, which works in the CIA environment (for details see Bontemps et al. 1999 and Kaas et al. 1999). This programme allows to discriminate astronomical sources from remaining low-level glitches or ghosts due to strong transients. For each source the photometric flux is the median flux obtained from all the readouts per sky position. An aperture integration of 9″ and sky emission subtraction were used, and the aperture correction based on observed point-spread function was applied. The adopted conversion factors 1mJy = 2.331 ADU/gain/s for LW2 and 1mJy = 1.97 ADU/gain/s for LW3 were taken from the latest version of CIA. The flux uncertaintes are estimated from the standard deviation around the median, and from the σ of the sky background. The detection limits for this survey are about 0.7 mJy and 1.3 mJy (1σ) for LW2 and LW3 respectively, except for the south-east region that are worse by a factor of ~ 2.

From the comparison of the ISOCAM coordinates with those of optical bright sources present in the region, we estimate the positional accuracy of the ISOCAM sources to be about $\pm$ 5″ in both directions. A more accurate astrometry within $\pm$ 1″ of the detected sources was made taking the coordinates of the identified ISOCAM sources from the DENIS survey (Cambrésy et al. 1998). In the following for all the detected sources we will use this last astrometry.

3. Results

Within the surveyed region of Cha I (0.59 sq.deg.) that contains the three reflection nebulae Ced 110, 111, and 112, 282 sources have been detected in LW2 (λ_{eff}=6.7 μm), and 103 of these sources were found also in LW3 (λ_{eff} =14.3 μm). All these detections have a S/N $\geq$3. We have identified 74 of the ISOCAM sources previously known as members of the cloud from Hα, X-ray and near–IR observations. In addition, using the DENIS survey of the region in I, J and K_s bands described by Cambrésy et al. (1998), yields that about 96% of the ISOCAM sources have a near–IR counterpart. A complete list of the 282 ISOCAM sources including the positions, the DENIS photometry and the ISOCAM flux densities is not reported here, but can be available upon request (persi@saturn.ias.rm.cnr.it). In a few cases the identification between ISOCAM and DENIS is uncertain because of the presence of more than one near-IR source surrounding the ISOCAM position. These sources are marked with an asterisk in the general table.

3.1. ISOCAM colour/magnitude diagram

As shown by Nordh et al. (1996) and Olofsson et al. (1999), the $m_{14.3}$ versus $m_{6.7}$-$m_{14.3}$ diagram, is a powerful tool to separate sources with and without IR excess in star forming regions. Using the following conversion flux densities to magnitude, $m_{6.7}$=-2.5log(F_ν(6.7)/83.4) and $m_{14.3}$=-2.5log(F_ν(14.3)/18.9), with F_ν given in Jy, we have derived the ISOCAM colour/magnitude plot for the 103 sources detected in both filters. This diagram for Cha I is reported in Fig. 1.

We can distinguish two different populations: one with colour indices around zero, in which the mid-IR emission is due to the photosphere of the star, and the other with a clear mid-IR

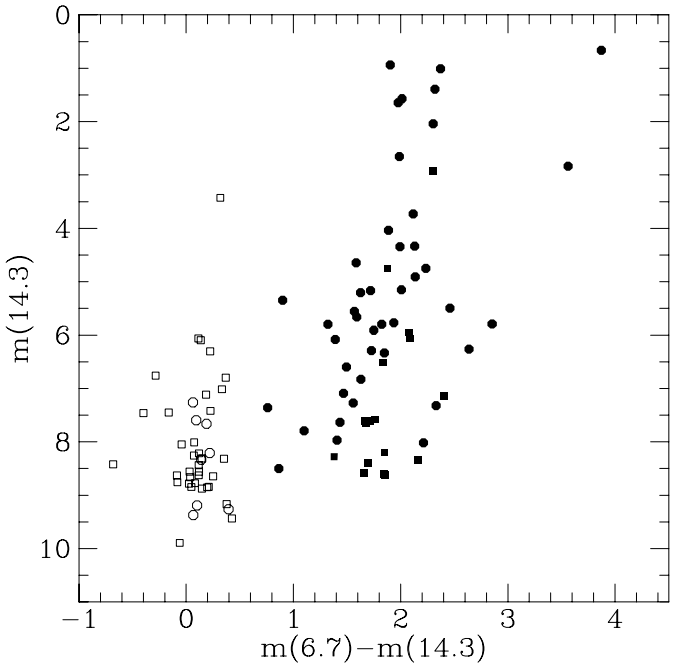

Fig. 1. Colour/magnitude plot for the ISOCAM sources in Cha I, detected in both filters. Filled and open circles represent known members in the cloud, while the open and filled squares are new detections.

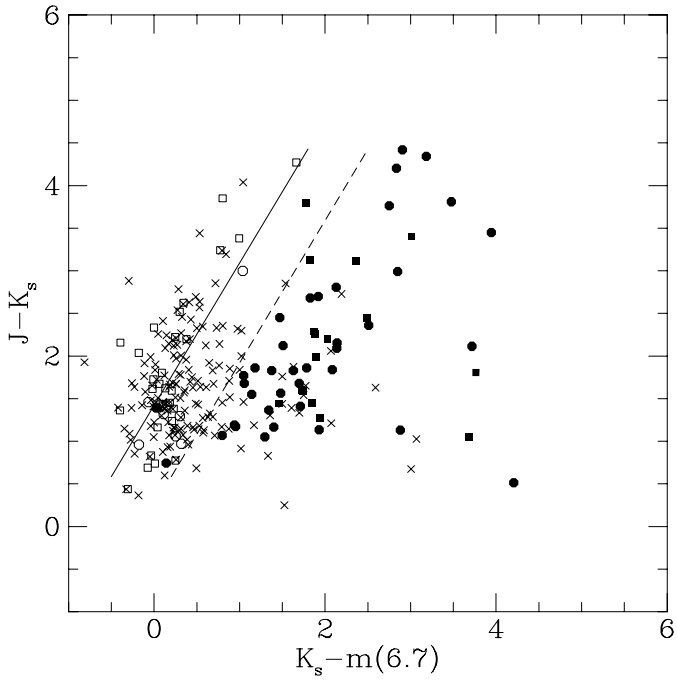

Fig. 2. J–K_s versus K_s–$m_{6.7}$ diagram of the ISOCAM sources. Symbols as Fig. 1. Crosses are sources detected only at LW2.

excess due mainly to the circumstellar dust material around the young stars. Skrutskie et al. (1990) analysed the ΔK vs ΔN plot (the logarithmic ratios of observed to photospheric fluxes at 2.2 and 10 μm) for 83 PMS stars in Taurus-Auriga, and found that their sample stars fell in two domains separated by a gap similar to that found in Fig. 1.

Most of the known members of Cha I show mid-IR excess (filled circles in Fig. 1), and only 8 (open circles in Fig. 1) have a mid–IR colour close to zero as expected for normal stars. The spread around this value is consistent with that expected from photometric uncertainty alone.

Of the 51 new sources detected at 6.7 and 14.3 μm, seventeen of these show also mid-IR excess (filled squares in Fig. 1), and the remainder have colour indices typical for normal stars (open squares in Fig. 1). The observed flux densities at 14.3 μm of the new sources with mid–IR excess are in general weaker than for the known members.

3.2. The J–K_s versus K_s–$m_{6.7}$ diagram

For 255 sources observed in J, K_s and 6.7 μm, we have obtained the colour/colour diagram J-K_s versus K_s–$m_{6.7}$ (Fig. 2). This diagram is useful also in separating the effects from intrinsic IR excess and from reddening. The continuous line in Fig. 2 represents the reddening line obtained from the reddening law of Rieke & Lebofsky (1985).

We consider here sources with intrinsic K_s-m(6.7) excess those lying to the right of the reddening band (dashed line in Fig. 2) obtained by shifting to the right the reddening line by an amount determined from the photometric errors. From Fig. 2 we see that background stars or stars without excess, scatter along the reddening line, while sources with red $m_{6.7}$ -$m_{14.3}$ colours (filled circles and filled squares in Fig. 2) are all, with only three exceptions, located to the right of the assumed reddening band. In addition, 24 sources detected only at 6.7 μm (crosses in Fig. 2) show also infrared excess. These sources are probably too faint to be detected at 14.3 μm. This analysis indicates that the colour/colour diagram obtained combining near–IR and LW2 photometry is a complementary way to add new members of the cloud.

The list including the positions, the near–IR photometry and the ISOCAM flux densities of the previously known members of Cha I with IR excess is reported in Table 1, while Table 2 gives the same parameters for the new sources with IR excess selected from the analysis of Fig. 1 and Fig. 2. The DENIS photometry is taken partially from Cambrésy et al. (1998) and from our own analysis of the DENIS images.

The sources ISO-ChaI-95 and ISO-ChaI-111 reported in Table 1 and identified by Neuhäuser & Comerón (1999) as a young brown dwarf (Cha Hα1), and a candidate brown dwarf (Cha Hα2), respectively, both show no near-IR excess while they possess a consistent mid–IR excess. Particularly interesting is the new detected source ISO-ChaI-86 observed with a strong mid–IR excess (see Table 2). From an inspection of the DENIS images and of the near–IR images collected at the 1.5 m telescope of Cerro Tololo (Gomez, private communication) no near-IR counterpart has been found. This suggests that the source located in the region of the reflection nebula Ced 110, could be a very embedded object with an infrared spectral index $\alpha_{\rm IR} \geq 1$.

3.3. Spatial distribution of the ISOCAM sources

Fig. 3 illustrates the spatial distribution of the ISOCAM sources found in Cha I superposed on the extinction map of Cambrésy et al. (1997) derived from the DENIS star counts in J band. Most of the 84 sources with mid–IR excess and excess in K_s–$m_{6.7}$ (filled circles in Fig. 3) are located in the densest part of the cloud ($A_V \approx$ 7-10) confirming their young nature. In particular, small clusters are observed towards the three reflection nebulae Ced 110, 111,and 112. ISOCAM sources without mid–IR excess (open circles in Fig. 3), and observed only at 6.7 μm without IR excess (plus signs in Fig. 3) are scattered uniformly through the cloud indicating that the majority of these are field stars. Only one extended source located in the northern part of ChaI has been found in our survey. This source coincides with the Herbig Ae star HD 97300, and has been studied in detail with ISOCAM photometric images by Siebenmorgen et al. (1998).

4. Discussion

We have identified from the previous analysis 34 new young stellar objects with circumstellar dust, belonging to the Chamaeleon I dark cloud (see Table 2). Including the 74 PMS stars previously identified, we found a total of 108 members in an area of 0.59 sq.deg. of Cha I. The sample is dominated by young stars with IR excess ($\sim$ 76%) probably Class I or Class II objects. This is essentially due to the fact that from our analysis, it is impossible to discriminate between field stars and members of the clouds without IR excess (Class III sources). In fact, these two groups of stars are located in the same area of the ISOCAM magnitude/colour and colour/colour diagrams (see Fig. 1 and Fig. 2). Therefore, optical spectroscopy, X-rays and proper motion surveys, are required to search for unidentified Class III sources. In the following we will discuss the luminosity funcion (LF) of the 108 identified members and give an infrared classification for the sources observed in the K_s and the 14.3 μm bands.

4.1. Luminosity function

For the 88 members of the cloud that are detected in both the I and J bands, we have derived the stellar luminosities according to the relationship:

$\log L(L_\odot)$ = 1.86 - 0.4(J-DM-A_J) - 0.4 BC_J

where J is the measured J magnitude, DM = 6.02 is the distance modulus, and A_J is:

$A_J = 0.8[(I-J) - (I-J)_0]$

This relation has been obtained using the Rieke & Lebofsky (1985) extinction law, and taking into account that the DENIS I filter is centered at 0.8 μm instead of 0.9 μm as adopted by Rieke & Lebosky. The intrinsic colours $(I-J)_0$ and the bolometric corrections in J, BC_J, are taken from Kenyon & Hartmann (1995). For the new detected sources and for the known members without any spectral classification, we have assumed a spectral type M2.5.

Comparing our calculated stellar luminosities with those of Lawson et al. (1996), we found, after correcting for the different distance adopted, an agreement within a factor of 2. In addition, we note that the luminosities derived for the new members detected by ISOCAM are on average lower than those of the previously identified members. This shows the importance of the ISOCAM survey in extending the study of the LF towards the lower end. Of course, a spectral classification is needed for these objects in order to confirm our estimated stellar luminosities.

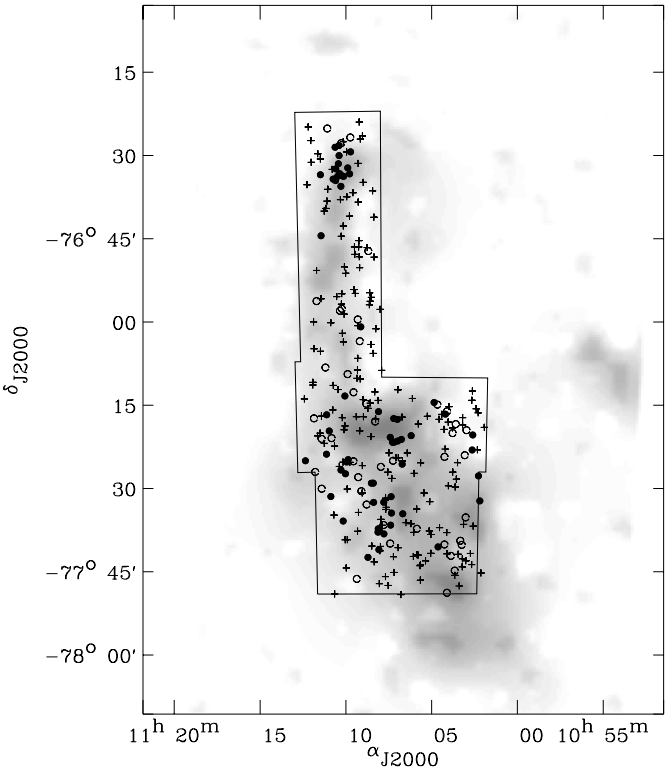

Fig. 3. Spatial distribution of the ISOCAM sources in Cha I superposed on the visual extinction map in magnitude steps of Cambrésy et al. (1997). The continuous line denotes the boundary of the ISOCAM survey. Filled circles indicate sources with mid–IR excess or excess in K_s–$m_{6.7}$, while open circles represent ISOCAM sources without mid–IR excess. Sources detected only at 6.7 μm without IR excess are indicated with a plus sign.

Table 3 and Table 4 give the stellar luminosities for the identified and not identified members of Cha I derived from the J magnitude. The spectral type of the identified members are taken from the literature.

In addition, we have derived for some of the members, the infrared spectral index $\alpha_{\rm IR}$ = dlog(λF_λ)/dlog(λ) calculated between 2.2 and 14.3 μm. This infrared spectral index is related, according to Lada (1987), to the evolution of low mass YSOs. The majority of the members in our sample have an infrared spectral index -1.6$\leq\alpha_{\rm IR}\leq$0.3 (see Table 3 and Table 4), indicating that, most likely, the population in the Cha I dark cloud is dominated by Class II YSOs in which the observed flat–spectrum is the consequence of accretion processes in a circumstellar disk.

The stellar luminosities calculated for the identified IR-excess members of Cha I with a good spectral classification,

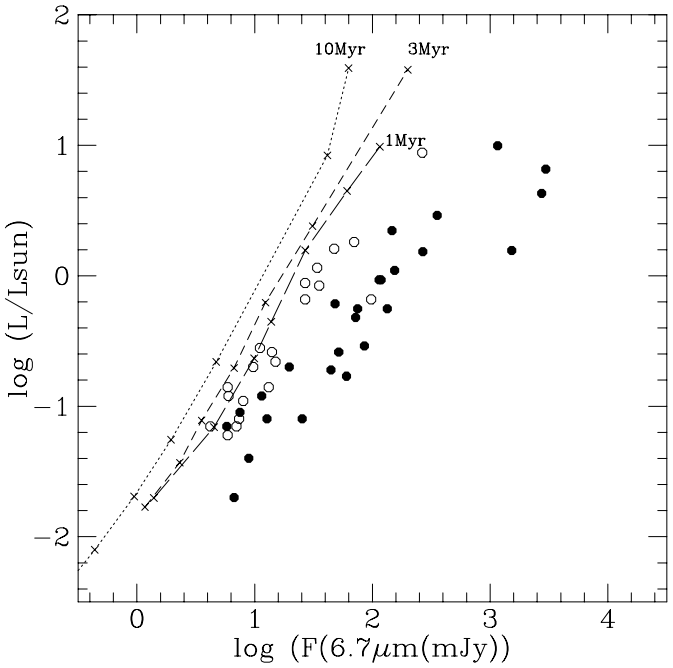

Fig. 4. Correlation between the ISOCAM flux densities at 6.7 μm and the L$\star$ computed for identified members. Stars with and without IR excess are represented by filled and open circles, respectively. The dotted and dashed lines show the locii of *bare* stars for 1, 3, and 10Myr, according to the evolutionary models by D'Antona & Mazzitelli (1998) computed for masses: 0.05, 0.1, 0.2, 0.4, 0.8, 1.6 and 2.5 $M_{\odot}$ (crosses).

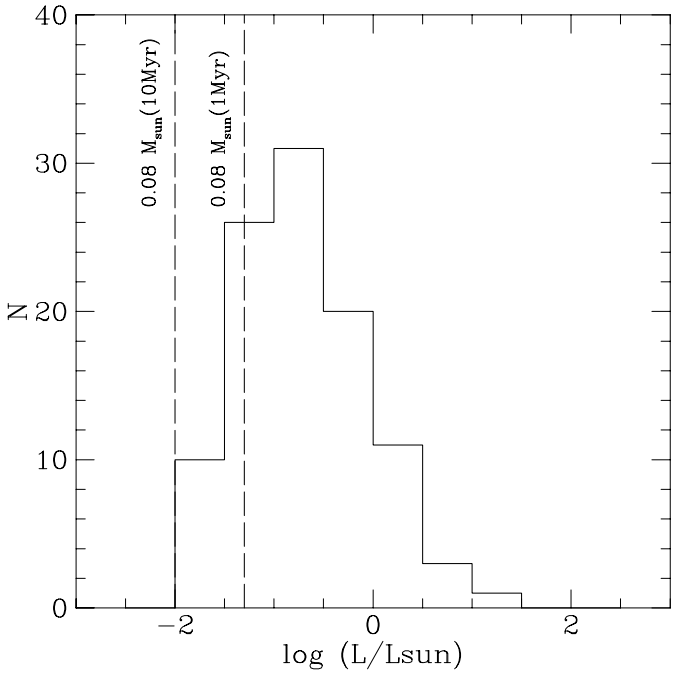

Fig. 5. Luminosity function of 108 members of the Chamaeleon I dark cloud.

correlate roughly with the 6.7 μm flux densities according to the relation log(L/$L_{\odot}$) = 0.83 log($F_{6.7}$(mJy))-1.93 (see Fig. 4). This correlation, due to the fact that Cha I is dominated by Class II sources, can be used in an empirical way to estimate the luminosities for 20 members without near–IR colours. This method has been applied by Bontemps et al. (2000), Olofsson et al. (1999) and Kaas et al. (2000) for ISOCAM sources in ρ Oph, RCrA, and Serpens, respectively.

Fig. 4 shows also that the stars without IR excess are located close to the theoretical relations for *bare* YSOs obtained for 1,3 and 10 Myr using the evolutionary models by D'Antona & Mazzitelli (1998), and assuming the blackbody spectral energy distributions for the given temperatures. Members with IR excess are, with a few exceptions, well to the right of these tracks.

The luminosity function (LF) for the 108 members of Chamaeleon I is presented in Fig. 5. The total uncertainty in deriving L$\star$ is expected to be about a factor of 2 for the luminosities derived from the near-IR colours, and to strongly depend on the extinction of the source. Larger errors are expected for luminosities obtained from the L$\star$–LW2 relation. In Fig. 5 are shown as dashed vertical lines the locations of the transition from stellar to subsellar masses for the two ages: 1 and 10 million years, based on the model of D'Antona & Mazzitelli (1998). Since the mean age of the Cha I population is of the order of 5 10^6 yr (Lawson et al. 1996), we conclude that a number of low luminosity objects detected in our survey are young brown dwarfs. This is also supported by the indipendent spectroscopic confirmation of some of them (Neuhäuser & Comerón (1999).

5. Conclusions

We have conducted a deep mid–infrared survey of a large portion (0.59 sq.deg.) of the Chamaeleon I dark cloud with ISOCAM at 6.7 and 14.3 μm. From the analysis of the ISOCAM data in combination with the DENIS near–infrared data, the following conclusions can be drawn:

1. A total of 282 point sources with a S/N$\geq$3 have been detected at 6.7 μm and 103 of these also detected at 14.3 μm. On the basis of the ISOCAM magnitude/colour diagram and the colour/colour diagram J-K_s versus K_s–$m_{6.7}$, we found 108 pre-main sequence stars in the region, of which 34 are new detections. Infrared excesses are present in 82 of these sources.

2. The spatial distribution of the mid–IR excess sources is mainly concentrated towards the densest part of Cha I, in proximity of the reflection nebulae Ced 110, 111, and 112. In addition, there are dense clumps in Cha I which do not seem to have young stars associated with them.

3. The spectral index $\alpha_{\rm IR}$ computed between 2.2 and 14.3 μm indicate that most of the sources with IR excess are Class II sources. Our analysis is not sufficient to discriminate Class III sources from field stars.

4. We have derived the stellar luminosities for 108 members of the cloud, from the observed J magnitudes and from the 6.7 μm flux densities. The derived luminosity function for this sample indicates the presence of a number of stars below the brown dwarf limit if their age is less than 10^7 yr. Optical spectroscopy is required for these objects in order to confirm the result.

In a forthcoming paper we will present a detailed study of the spectral energy distribution including new near–IR photometry and the present ISOCAM flux densities of the very low-mass objects found in this survey.

Acknowledgements. We are grateful to the referee F. Comerón for suggestions, which helped to improve the contents of this paper.

References

Abergel A., Bernard J.P., Boulanger F., et al., 1996, A&A 315, L329
Alcalá J.M., 1994, Ph.D. Thesis, Ruprecht-Karls-Universität, Heidelberg
Baud B., Beintema D., Wesselius P., et al., 1984, ApJ 278, L53
Bontemps S., Nordh L., Olofsson G., et al., 1999, In: The Universe as seen by ISO. ESA SP-427, p. 475
Bontemps S., Nordh L., Olofsson G., et al., 2000, A&A to, be submitted
Cambrésy L., Epchtein N., Copet E., et al., 1997, A&A 324, L5
Cambrésy L., Copet E., Epchtein N., et al., 1998, A&A 338, 977
Cesarsky C.J., Abergel A., Agnése P., et al., 1996, A&A 315, L32
Comerón F., Rieke G.H., Neuhäuser R., 1999, A&A 343, 477
D'Antona F., Mazzitelli I., 1998, Mem. Soc. Astron. Ital. 68, 807
Gauvin L.S., Strom K.M., 1992, ApJ 385, 317
Hartigan P., 1993, AJ 105, 1511
Huenemoerder D.P., Lawson W.A., Feigelson E.D., 1994, MNRAS 271, 967
Jones T., Hyland A., Harvey P., et al., 1985, AJ 90, 1191
Kaas A.A., Olofsson G., Bontemps S., et al., 1999, In: The Universe as seen by ISO. ESA SP-427, p. 493
Kaas A.A., et al., 2000, in preparation
Kenyon S.J., Hartmann L., 1995, ApJS 101, 117
Kessler M.F., Steinz J.A., Anderegg M.E., et al., 1996, A&A 315, L27
Lada C.J., 1987, In: Star Forming Regions. IAU 115, p. 1
Lawson W.A., Feigelson E.D., Huenemoerder D.P., 1996, MNRAS 280, 1071
Neuhäuser R., Comerón F., 1999, A&A 350, 612
Nordh L., Olofsson G., Abergel A., et al., 1996, A&A 315, L185
Nordh L., Olofsson G., Bontemps S., et al., 1998, In: Star formation with the Infrared Space Observatory. ASP Conf. Ser. vol. 132, p. 127
Olofsson G., Huldtgren M., Kaas A.A., et al., 1999, A&A 350, 883
Ott S., Abergel A., Altieri B., 1997, In: Astronomical Data Analysis Software and Systems. ASP Conf. Ser. vol. 125, p. 34
Persi P., Marenzi A.R., Kaas A.A., et al., 1999, AJ 117, 439
Prusti T., Clark F., Whittet D., et al., 1991, MNRAS 251, 303
Prusti T., Whittet D.C.B., Wesselius P.R., 1992, MNRAS 254, 361
Rieke G.K., Lebofsky M.J., 1985, ApJ 288, 618
Schwartz R., 1991, In: Reipurth B. (ed.) Scientific Report no. 11, ESO, p. 93
Siebenmorgen R., Natta A., Krugel E., Prusti T., 1998, A&A 339, 134
Starck J.L., Murtagh F., Pirenne B., Albrecht M., 1996, PASP 108, 446
Starck J.L., Abergel A., Aussel H., et al., 1999, A&AS 134, 135
Skrutskie M.F., Dutkevitch D., Strom S.E., et al., 1990, AJ 99, 1187
Whittet D.C.B., Prusti T., Franco G.A.P., et al., 1997, A&A 327, 1194